3 Elements of contact mechanics

3.1. Introduction

There is a group of machine components whose functioning depends upon rolling and sliding motion along surfaces while under load. Both surfaces are usually convex, so that the area through which the load is transferred is very small, even after some surface deformation, and the pressures and local stresses are very high. Unless logically designed for the load and life expected of it, the component may fail by early general wear or by local fatigue failure. The magnitude of the damage is a function of the materials and by the intensity of the applied load or pressure, as well as the surface finish, lubrication and relative motion.

The intensity of the load can be determined from equations which are functions of the geometry of the surfaces, essentially the radii of curvature, and the elastic constants of the materials. Large radii and smaller moduli of elasticity, give larger contact areas and lower pressures. Careful alignment, smoother surfaces, and higher strength and oil viscosity minimize failures.

In this chapter, presentation and discussion of *contact mechanics* is confined, for reasons of space, to the most technically important topics. However, a far more comprehensive treatment of contact problems in a form suitable for the practising engineer is given in the ESDU tribology series. The following items are recommended:

ESDU-78035, Contact phenomena I; stresses, deflections and contact dimensions for normally loaded unlubricated elastic components;

ESDU-84017, Contact phenomena II; stress fields and failure criteria in concentrated elastic contacts under combined normal and tangential loading;

ESDU-85007, Contact phenomena III; calculation of individual stress components in concentrated elastic contacts under combined normal and tangential loading.

Although a fairly comprehensive treatment of thermal effects in surface contacts is given here it is appropriate, however, to mention the ESDU tribology series where thermal aspects of bearings, treated as a system are presented, and network theory is employed in an easy to follow step-by-step procedure. The following items are esentially recommended for the practising designer:

ESDU-78026, Equilibrium temperatures in self-contained bearing assemblies;
Part I - outline of method of estimation;

ESDU-78027, Part II - first approximation to temperature rise;
ESDU-78028, Part III - estimation of thermal resistance of an assembly;
ESDU-78029, Part IV - heat transfer coefficient and joint conductance.

Throughout this chapter, references are made to the appropriate ESDU item number, in order to supplement information on contact mechanics and thermal effects, offer alternative approach or simply to point out the source of technical data required to carry out certain analysis.

3.2. Concentrated and distributed forces on plane surfaces

The theory of contact stresses and deformations is one of the more difficult topics in the theory of elasticity. The usual approach is to start with forces applied to the plane boundaries of semi-infinite bodies, i.e. bodies which extend indefinitely in all directions on one side of the plane. Theoretically this means that the stresses which radiate away from the applied forces and die out rapidly are unaffected by any stresses from reaction forces or moments elsewhere on the body.

A concentrated force acts at point O in case 1 of Table 3.1. At any point Q there is a resultant stress q on a plane perpendicular to OZ, directed through O and of magnitude inversely proportional to (r^2+z^2), or the

Table 3.1

Loading case	Pictorial	Stress and deflection
1. Point	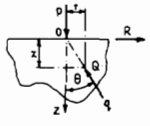	$q=\sqrt{\sigma_z^2+\tau_{rz}^2}\quad \frac{3}{2\pi}\frac{P\cos^2\theta}{(r^2+z^2)}$ $w=\frac{1-\nu^2}{\pi E}\frac{P}{r}$ at surface
2. Line	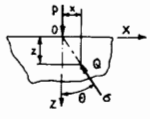	$\sigma=\frac{2}{\pi}\frac{(P/l)\cos\theta}{\sqrt{x^2+z^2}}$
3. Knife edge or pivot	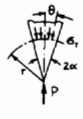	$\sigma_r=-\frac{(P/L)\cos\theta}{r(\alpha+\frac{1}{2}\sin 2\alpha)}$
4. Uniform distributed load p over circle of radius a	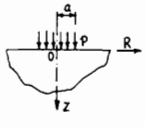	with $\nu=0.3$ at point O $\sigma_z=-p, \sigma_r=\sigma_\theta=-0.8p$ $w_m=\frac{2(1-\nu^2)pa}{E}=2\eta pa$ $T_m=0.33p$ at $z=0.638a$
5. Rigid cylinder ($E_1 \gg E_2$)	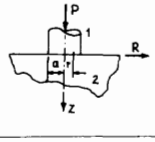	$(\sigma_z)_{z=0}=-p=-\frac{P}{2\pi a\sqrt{a^2-r^2}}$ $w=\frac{(1-\nu^2)P}{2E_2 a}=\frac{\eta_2 P}{2a}$

square of the distance OQ from the point of load application. This is an indication of the rate at which stresses die out. The deflection of the surface at a radial distance r is inversely proportional to r, and hence, is a hyperbola asymptotic to axes OR and OZ. At the origin, the stresses and deflections theoretically become infinite, and one must imagine the material near O cut out, say, by a small hemispherical surface to which are applied distributed forces that are statistically equivalent to the concentrated force P. Such a surface is obtained by the yielding of the material.

An analogous case is that of concentrated loading along a line of length l (case 2). Here, the force is P/l per unit length of the line. The result is a normal stress directed through the origin and inversely proportional to the first power of distance to the load, not fading out as rapidly. Again, the stress approaches infinite values near the load. Yielding, followed by work-hardening, may limit the damage. Stresses in a knife or wedge, which might be used to apply the foregoing load, are given under case 3. The solution for case 2 is obtained when $2\alpha = \pi$, or when the wedge becomes a plane.

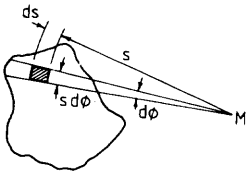

Figure 3.1

In the deflection equation of case 1, we may substitute for the force P, an expression that is the product of a pressure p, and an elemental area, such as the shaded area in Fig. 3.1. This gives a deflection at any point, M, on the surface at a distance $r = s$ away from the element, namely

$$dw = \frac{(1-\nu^2)}{\pi E} \frac{p(s\,d\phi)\,ds}{s} = \frac{(1-\nu^2)p\,ds\,d\phi}{\pi E},$$

where ν is the Poisson ratio. The total deflection at M is the superposition or integration over the loaded area of all the elemental deflections, namely

$$w = \frac{(1-\nu^2)}{\pi E} \int\int p\,ds\,d\phi = \frac{\eta}{\pi} \int\int p\,ds\,d\phi, \tag{3.1}$$

where η is an elastic constant $(1-\nu^2)/E$. If the pressure is considered uniform, as from a fluid, and the loaded area is a circle, the resulting deflections, in terms of elliptic integrals, are given by two equations, one for M outside the circle and one for M inside the circle. The deflections at the centre are given under case 4 of Table 3.1. The stresses are also obtained by a superposition of elemental stresses for point loading. Shear stress is at a maximum below the surface.

If a rod in the form of a punch, die or structural column is pressed against the surface of a relatively soft material, i.e. one with a modulus of elasticity much less than that of the rod, the rod may be considered rigid, and the distribution of deflection is initially known. For a circular section, with deflection w constant over the circle, the results are listed in case 5. The pressure p is least at the centre, where it is $0.5p_{avg}$, and it is infinite at the edges. The resultant yielding at the edges is local and has little effect on the general distribution of pressure. For a given total load, the deflection is inversely proportional to the radius of the circle.

3.3. Contact between two elastic bodies in the form of spheres

When two elastic bodies with convex surfaces, or one convex and one plane surface, or one convex and one concave surface, are brought together in point or line contact and then loaded, local deformation will occur, and the point or line will enlarge into a surface of contact. In general, its area is bounded by an ellipse, which becomes a circle when the contacting bodies are spheres, and a narrow rectangle when they are cylinders with parallel axes. These cases differ from those of the preceding section in that there are two elastic members, and the pressure between them must be determined from their geometry and elastic properties.

The solutions for deformation, area of contact, pressure distribution and stresses at the initial point of contact were made by Hertz. They are presented in ESDU 78035 in a form suitable for engineering application. The maximum compressive stress, acting normal to the surface is equal and opposite to the maximum pressure, and this is frequently called the Hertz stress. The assumption is made that the dimensions of the contact area are small, relative to the radii of curvature and to the overall dimensions of the bodies. Thus the radii, though varying, may be taken as constant over the very small arcs subtending the contact area. Also, the deflection integral derived for a plane surface, eqn (3.1), may be used with very minor error. This makes the stresses and their distribution the same in both contacting bodies.

The methods of solution will be illustrated by the case of two spheres of different material and radii R_1 and R_2. Figure 3.2 shows the spheres before and after loading, with the radius a of the contact area greatly exaggerated for clarity. Distance $z = R - R\cos\gamma \approx R - R(1 - \gamma^2/2 + \cdots) \approx R\gamma^2 2 \approx r^2/2R$ because $\cos\gamma$ may be expanded in series and the small angle $\gamma \approx r/R$. If points M_1 and M_2 in Fig. 3.2 fall within the contact area, their approach distance M_1M_2 is

$$z_1 + z_2 = \frac{r^2}{2}\left(\frac{1}{R_1} + \frac{1}{R_2}\right) = Br^2, \tag{3.2}$$

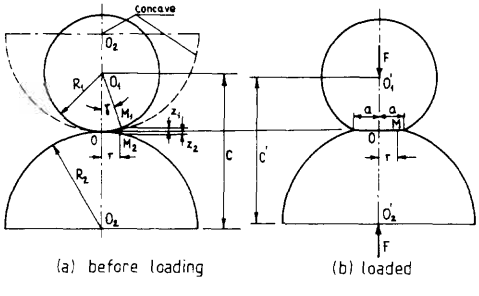

Figure 3.2

where B is a constant $(1/2)(1/R_1 + 1/R_2)$. If one surface is concave, as indicated by the dotted line in Fig. 3.2, the distance is $z_1 - z_2 = (r^2/2)(1/R_1 - 1/R_2)$ which indicates that when the contact area is on the inside of a surface the numerical value of its radius is to be taken as negative in all equations derived from eqn (3.1).

The approach between two relatively distant and strain-free points, such as Q_1 and Q_2, consists not only of the surface effect z_1+z_2, but also of the approach of Q_1 and Q_2 relative to M_1 and M_2, respectively, which are the deformations w_1 and w_2 due to the, as yet, undetermined pressure over the contact area. The total approach or deflection δ, with substitution from eqn (3.1) and (3.2), is

$$\delta=(z_1+z_2)+(w_1+w_2)=Br^2+(1/\pi)(\eta_1+\eta_2)\int\int p\,\mathrm{d}s\,\mathrm{d}\phi,$$

where

$$\eta_1=(1-\nu_1^2)/E_1 \qquad \text{and} \qquad \eta_2=(1-\nu_2^2)/E_2.$$

With rearrangement,

$$\frac{\eta_1+\eta_2}{\pi}\int\int p\,\mathrm{d}s\,\mathrm{d}\phi=\delta-Br^2. \tag{3.3}$$

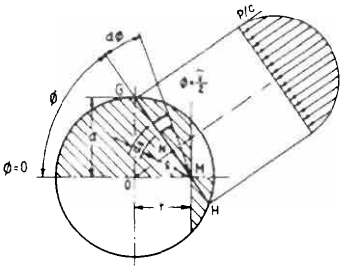

Figure 3.3

For symmetry, the area of contact must be bounded by a circle, say of radius a, and Fig. 3.3 is a special case of Fig. 3.1. A trial will show that eqn (3.3) will be satisfied by a hemispherical pressure distribution over the circular area. Thus the peak pressure at centre O is proportional to the radius a, or $p_0=ca$. Then, the scale for plotting pressure is $c=p_0/a$. To find w_1 and w_2 at M in eqn (3.3), an integration, $p\,\mathrm{d}s$, must first be made along a chord GH, which has the half-length $\mathrm{GN}=(a^2-r^2\sin^2\phi)^{\frac{1}{2}}$. The pressure varies as a semicircle along this chord, and the integral equals the pressure scale c times the area A under the semicircle, or

$$\int p\cdot\mathrm{d}s=cA=\frac{p_0\pi}{a}\frac{}{2}(a^2-r^2\sin^2\phi).$$

By a rotation of line GH about M from $\phi=0$ to $\phi=\pi/2$ (half of the contact circle), the shaded area of Fig. 3.3, is covered. Doubling the integral completes the integration in eqn (3.3), namely

$$\frac{p_0(\eta_1+\eta_2)}{a}\int_0^{\frac{\pi}{2}}(a^2-r^2\sin^2\phi)\,\mathrm{d}\phi=\delta-Br^2,$$

whence

$$\frac{p_0\pi}{4a}(\eta_1+\eta_2)(2a^2-r^2)=\delta-Br^2. \tag{3.4}$$

Now the approach δ of centres Q_1 and Q_2, is independent of the particular points M and radius r, chosen in the representation by which eqn (3.4) was obtained. To make the equation independent of r, the two r^2 terms must be equal, whence it follows that the two constant terms are equal. The r^2 terms, equated and solved for a, yield the radius of the contact area

$$a=\frac{p_0\pi(\eta_1+\eta_2)}{4B}. \tag{3.5}$$

The two constant terms when equated give

$$\delta = \frac{p_0 \pi(\eta_1 + \eta_2)a}{2}. \tag{3.6}$$

The integral of the pressure over the contact area is equal to the force P by which the spheres are pressed together. This integral is the pressure

Table 3.2

Loading case	Pictorial	Area, Pressure, Approach
1. Spheres or sphere and plane	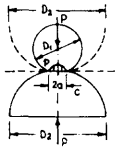	$a = 0.721[P(\eta_1+\eta_2)D_1D_2/(D_1+D_2)]^{\frac{1}{3}} = c/2$ $P_0 = 1.5P/\pi a^2 = 1.5p_{avg} = -(\sigma_c)_{max}$ max $\tau = \frac{1}{3}p_0$, at depth $0.638a$ max $\sigma_t = (1-2\nu)p_0/3$ at radius a $\delta = 1.04[(\eta_1+\eta_2)^2P^2(D_1+D_2)/D_1D_2]^{\frac{1}{3}}$
2. Cylindrical surfaces with parallel axes	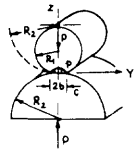	$b = 1.13\sqrt{(P/l)(\eta_1+\eta_2)R_1R_2/(R_1+R_2)} = c/2$ $p_0 = 2P/\pi bl = 1.273p_{avg} = -(\sigma_c)_{max}$ if $\nu = 0.30$ max $\tau = 0.304p_0$ at depth $0.786b$ if $\eta_1 = \eta_2 = \eta$ $\delta = 0.638(P/l)\eta\left[\frac{2}{3} + \ln\frac{2R_1}{b} + \ln\frac{2R_2}{b}\right]$
3. General case	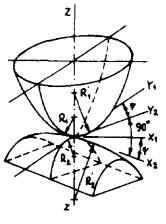	$b = \beta\left[\frac{3P(\eta_1+\eta_2)}{4(B+A)}\right]^{\frac{1}{3}}$ and $a = b/k$ $B+A = \frac{1}{2}\left[\frac{1}{R_1}+\frac{1}{R_1'}+\frac{1}{R_2}+\frac{1}{R_2'}\right]$ $B-A = \frac{1}{2}\left[\left(\frac{1}{R_1}-\frac{1}{R_1'}\right)^2+\left(\frac{1}{R_2}-\frac{1}{R_2'}\right)^2 + 2\left(\frac{1}{R_1}-\frac{1}{R_1'}\right)\left(\frac{1}{R_2}-\frac{1}{R_2'}\right)\cos 2\psi\right]^{\frac{1}{2}}$ at $x = y = z = 0$ $p_0 = 1.5P/\pi ab = 1.5p_{avg} = -(\sigma_c)_{max}$ $\sigma_x = -2\nu p_0 - (1-2\nu)\,p_0\frac{b}{a+b}$ $\sigma_y = -2\nu p_0 - (1-2\nu)p_0\frac{a}{a+b}$ $\delta = \lambda[P^2(\eta_1+\eta_2)^2(B+A)]^{\frac{1}{3}}$

β, κ, λ are constants and obtained from appropriate diagrams

$$\eta_1 = \frac{1-\nu_1^2}{E_1} \text{ and } \eta_2 = \frac{1-\nu_2^2}{E_2}$$

scale times the volume under the hemispherical pressure plot, or

$$\frac{p_0}{a}\left(\tfrac{2}{3}\pi a^3\right) = P$$

and the peak pressure has the value

$$p_0 = 1.5P/\pi a^2 = 1.5p_{avg}. \tag{3.7}$$

Substitution of eqn (3.7) and the value of B below eqn (3.2) gives to eqns (3.5) and (3.6) the forms shown for case 1 of Table 3.2. If both spheres have the same elastic modulus $E_1 = E_2 = E$, and the Poisson ratio is 0.30, a simplified set of equations is obtained. With a ball on a plane surface, $R_2 = \infty$, and with a ball in a concave spherical seat, R_2 is negative.

It has taken all this just to obtain the pressure distribution on the surfaces. All stresses can now be found by the superposition or integration of those obtained for a concentrated force acting on a semi-infinite body. Some results are given under case 1 of Table 3.2. An unusual but not unexpected result is that pressures, stresses and deflections are not linear functions of load P, but rather increase at a less rapid rate than P. This is because of the increase of the contact or supporting area as the load increases. Pressures, stresses and deflections from several different loads cannot be superimposed because they are non-linear with load.

3.4. Contact between cylinders and between bodies of general shape

Equations for cylinders with parallel axes may be derived directly, as shown for spheres in Section 3.3. The contact area is a rectangle of width $2b$ and length l. The derivation starts with the stress for line contact (case 2 of Table 3.1). Some results are shown under case 2 of Table 3.2. Inspection of the equations for semiwidth b, and peak pressure p_0, indicates that both increase as the square root of load P. The equations of the table, except that given for δ, may be used for a cylinder on a plane by the substitution of infinity for R_2. The semiwidth b, for a cylinder on a plane becomes $1.13[(P/l)(\eta_1 + \eta_2)R_1]^{\frac{1}{2}}$. All normal stresses are compressive, with σ_y and σ_z equal at the surface to the contact pressure p_0. Also significant is the maximum shear stress τ_{yz}, with a value of $0.304p_0$ at a depth $0.786b$.

Case 3 of Table 3.2 pictures a more general case of two bodies, each with one major and one minor plane of curvature at the initial point of contact. Axis Z is normal to the tangent plane XY, and thus the Z axis contains the centres of the radii of curvature. The minimum and maximum radii for body 1 are R_1 and R_1', respectively, lying in planes Y_1Z and X_1Z. For body 2, they are R_2 and R_2', lying in planes Y_2Z and X_2Z, respectively. The angle between the planes with the minimum radii or between those with the maximum radii is ψ. In the case of two crossed cylinders with axes at 90°, such as a car wheel on a rail, $\psi = 90°$ and $R_1' = R_2' = \infty$. This general case was solved by Hertz and the results may be presented in various ways. Here, two sums $(B + A)$ and $(B - A)$, obtained from the geometry and defined under case 3 of Table 3.2 are taken as the basic parameters. The area of contact is an ellipse with a minor axis $2b$ and a major axis $2a$. The distribution of pressure is that of an ellipsoid built upon these axes, and the peak pressure is

1.5 times the average value $P/\pi ab$. However, for cylinders with parallel axes, the results are not usable in this form, and the contact area is a rectangle of known length, not an ellipse. The principal stresses shown in the table occur at the centre of the contact area, where they are maximum and compressive. At the edge of the contact ellipse, the surface stresses in a radial direction (along lines through the centre of contact) become tensile. Their magnitude is considerably less than that of the maximum compressive stresses, e.g. only $0.133p_0$ with two spheres and $\nu = 0.30$ by an equation of case 1, Table 3.2, but the tensile stresses may have more significance in the initiation and propagation of fatigue cracks. The circumferential stress is everywhere equal to the radial stress, but of opposite sign, so there is a condition of pure shear. With the two spheres $\tau = 0.133p_0$. Forces applied tangentially to the surface, such as by friction, have a significant effect upon the nature and location of the stresses. For example, two of the three compressive principal stresses immediately behind the tangential force are changed into tensile stresses. Also, the location of the maximum shear stress moves towards the surface and may be on it when the coefficient of friction exceeds 0.10.

More information on failure criteria in contacts under combined normal and tangential loading can be found in ESDU-84017.

3.5. Failures of contacting surfaces

There are several kinds of surface failures and they differ in action and appearance. Indentation (yielding caused by excessive pressure), may constitute failure in some machine components. Non-rotating but loaded ball-bearings can be damaged in this way, particularly if vibration and therefore inertia forces are added to dead weight and static load. This may occur during shipment of machinery and vehicles on freight cars, or in devices that must stand in a ready status for infrequent and short-life operations. The phenomena is called false brinelling, named after the indentations made in the standard Brinell hardness test.

The term, *surface failure*, is used here to describe a progressive loss of quality by the surface resulting from shearing and tearing away of particles. This may be a flat spot, as when a locked wheel slides on a rail. More generally the deterioration in surface quality is distributed over an entire active surface because of a combination of sliding and rolling actions, as on gear teeth. It may occur in the presence of oil or grease, where a lubricating film is not sufficiently developed, for complete separation of the contacting surfaces. On dry surfaces, it may consist of a flaking of oxides. If pressures are moderate, surface failures may not be noticeable until loose particles develop. The surface may even become polished, with machining and grinding marks disappearing. The generation of large amounts of particles, may result from misalignments and unanticipated deflections, on only a portion of the surface provided to take the entire load. This has been observed on the teeth of gears mounted on insufficiently rigid shafts, particularly when the gear is overhung. Rapid deterioration of surface quality may occur from insufficient lubrication, as on cam shafts, or from negligence in lubrication and protection from dirt.

A type of surface failure, particularly characteristic of concentrated

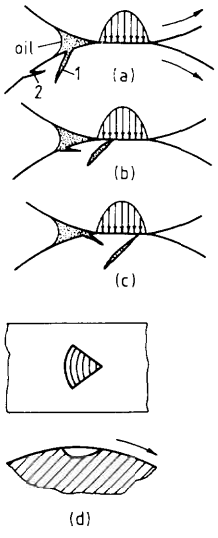

Figure 3.4

contacts, consists of fatigue cracks which progress into and under the surface, and particles which then fall out of the surface. The holes resulting from this process are called pits or spalls. This pitting occurs on convex surfaces, such as gear teeth, rolling element bearings and cams. It is a well-established fact that the maximum shearing stress occurs below the surfaces of bodies which are in contact. Hence, at one time, it was strongly held that the crack forming a pit started at this point of maximum shear stress, then progressed outwards. Data from pure rolling tests disclosed, however, that the cracks commonly started at the surface and progressed only in the presence of oil. A good penetrant, filling any fine cracks present, acted as a hydraulic wedge. Experiments also revealed that only cracks with their lips facing the approaching load would progress to failure.

In Fig. 3.4, a crack, 1, filled with oil, approaches the loading zone and has its lip sealed off. As the full length of the crack comes under the load, oil in the crack cannot escape, and high hydraulic pressure results. After repeated occurrence of this process, high stress from stress concentration along the root of the crack to spread by fatigue. Eventually, the crack will progress towards the surface, favouring the most highly stressed regions. Then, a particle will fall out, exposing a pit with the typical lines of progressive cracking, radiating from the pointed lip. The pit may look much as though it were moulded from a tiny sea shell, with an arrowhead point of origin. Pit depths may vary from a few microns to about 1 mm, with lengths from two to four times their depths.

Cracks facing away from the approaching zone of loading, such as crack 2 (Fig. 3.4), will not develop into pits. The root of the crack first reaches the loaded area and the oil in the crack is squeezed out by the time its lip is sealed off. A more viscous oil reduces or eliminates pitting, either by not penetrating into fine cracks, or by forming an oil film thick enough to prevent contact between asperities.

There are several possible causes for the initial surface cracks, which only need to be microscopic or even submacroscopic. Machining and grinding are known to leave fine surface cracks, either from a tearing action or from thermal stresses. Polishing inhibits pitting, presumably by the removal of these cracks. Along the edges of spherical and elliptical contact areas a small tensile stress is present under static and pure-rolling conditions. Tangential forces caused by sliding combined with rolling, as on gear teeth, add tensile stresses to the above and to the rectangular contact area of cylinders. Surface inclusions at the tensile areas create stress concentrations and add to the chance that the repeated tensile stresses will initiate cracks. Sometimes a piece that has dropped out of a pit passes through the contact zone, making a shallow indentation probably with edge cracks. Sometimes the breaking out of material continues rapidly in a direction away from the arrowhead point of origin, increasing in width and length. It is then called spalling. Spalling occurs more often in rolling-element bearings than in gears, sometimes covering more than half the width of a bearing race. Propagation of the crack from the surface is called a point-surface origin mode of failure. There might be so-called inclusion-origin failure. Inclu-

sions are non-metallic particles that are formed in, and not eliminated from, the melt in the refining process. They may be formed during the deoxidization of steel or by a reaction with the refractory of the container. The inclusion does not bond with the metal, so that essentially a cavity is present with a concentration of stress. The usual way to detect inclusions is by a magnetic particle method. A crack, starting at the inclusion, may propagate through the subsurface region for some distance, or the crack may head for the surface. If cracks on the surface form, further propagation may be by hydraulic action, with a final appearance similar to that from a point-surface origin. The damaged area is often large. It is well known that bearings made from vacuum-melted steel, and therefore a cleaner, more oxide-free steel, are less likely to fail and may be given higher load ratings.

There are three other types of failure which usually occur in heavily loaded roller bearings in test rigs. Geometric stress concentration occurs at the ends of a rectangular contact area, where the material is weaker without side support. Slight misalignment, shaft slope or taper error will move much of the load to one of the ends. In peeling, fatigue cracks propagate over large areas but at depths of 0.005 to 0.01 mm. This has been attributed to loss of hydrodynamic oil film, particularly when the surface finish has many asperities which are greater than the film thickness under the conditions of service. Subcase fatigue occurs on carburized elements where the loads are heavy, the core is weak and the case is thin, relative to the radii of curvature in contact. Cracks initiate and propagate below the effective case depth, and cracks break through to the surface at several places, probably from a crushing of the case due to lack of support.

3.6. Design values and procedures

Previous investigations, some of which are published, have not produced a common basis on which materials, properties, component configuration, operating conditions and theory may be combined to determine dimensions for a satisfactory life of concentrated contacts. The investigations indicate that much progress is being made, and they do furnish a guide to conditions and changes for improvement. Most surface-contact components operate satisfactorily, and their selection is often based on a nominal Hertz pressure determined from experience with a particular component and material, or a selection is made from the manufacturers tables based on tests and experience with their components. The various types of stresses, failures and their postulated causes, including those of subsurface origin, are all closely related to the maximum contact pressure calculated by the Hertz equations. If an allowable maximum Hertz pressure seems large compared with other physical properties of the particular material, it is because it is a compressive stress and the other two principal stresses are compressive. The shear stresses and tensile stresses that may initiate failures are much smaller. Also, the materials used are often hardened for maximum strength. Suggestions for changes in contact-stress components by which their load or life may be increased are:

1. larger radii or material of a lower modulus of elasticity to give larger contact area and lower stress;